

High-Performance Discrete Amplifier Based on a Second-Order Fiber Raman Oscillator

Stefano Faralli, Pilhan Kim, Claudia Cantini, Gabriele Bolognini, Giovanni Sacchi, Namkyoo Park, and Fabrizio Di Pasquale, *Member, IEEE*

Abstract—We propose a second-order counterpumped Raman ring fiber oscillator for high gain and low noise discrete Raman amplification with enhanced robustness to wavelength-division-multiplexing channels add-drop operations. Bit-error-rate measurement at 10 Gb/s shows negligible penalties up to 20-dB net gain.

Index Terms—Optical communication systems, Raman amplifiers, Rayleigh scattering, relative intensity noise (RIN).

I. INTRODUCTION

DISCRETE Raman amplifiers (DRAs) have been intensively studied for wavelength-division-multiplexing (WDM) system and network applications, with their fascinating properties of wide gain bandwidth at any wavelength, low noise, simple configuration, and high robustness to add-drop operations, overwhelming the traditional doped fiber amplifiers [1]. Furthermore, the recent advance of highly nonlinear fiber (HNLF) has enabled us to achieve a significant enhancement in Raman gain efficiency, overcoming their main drawback—the requirement of high-cost pump with high output power.

One of the approaches for the implementation of highly efficient and practical DRA includes a Raman fiber oscillator (RFO) [2]. By introducing high reflectivity fiber Bragg gratings (FBGs) at 1450 nm (one Raman Stokes away from the pump at 1360 nm), a resonant cavity is formed to generate laser, then providing gain for WDM signals in *C*-band. This oscillating configuration has been reported to be advantageous over conventional DRAs in terms of signal double Rayleigh scattering (DRS) noise, cross-phase modulation, saturation, and transient behaviors [2]. Although excellent in terms of above amplifier performance figures, the bit-error-rate (BER) measurements with this RFO configuration have shown large receiver power penalties due to relative intensity noise (RIN) transfer from lasing light at 1450 nm to the signal at 1550 nm, seriously degrading the transmission system performance. In this letter, we propose an alternative scheme based on a second-order counterpumped Raman ring fiber oscillator (RRFO), which

Manuscript received June 7, 2005; revised June 28, 2005. This work was supported in part by the Italian Ministry of Foreign Affairs (MAE) and in part by the Korean Ministry of Science and Technology.

S. Faralli, C. Cantini, G. Bolognini, and F. Di Pasquale are with Scuola Superiore Sant'Anna di Studi Universitari e Perfezionamento, Pisa 56123, Italy (e-mail: stefano.faralli@cni.it; fabrizio.dipasquale@cni.it).

P. Kim and N. Park are with the Optical Communication Systems Laboratory, Seoul National University, Seoul 151-742, Korea (e-mail: phkim@stargate.snu.ac.kr; nkpark@plaza.snu.ac.kr).

G. Sacchi is with Laboratorio Nazionale di Reti Fotoniche, CNIT, Pisa 56123, Italy (e-mail: giovanni.sacchi@cni.it).

Digital Object Identifier 10.1109/LPT.2005.857235

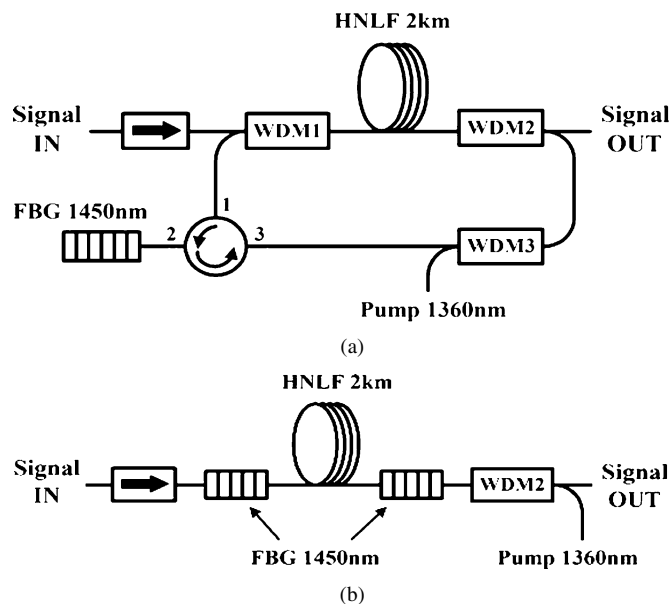


Fig. 1(a). Schematic diagram of the RRFO. (b) Schematic diagram of the RFO.

outperforms both RFO-based amplifiers and conventional DRAs, ensuring negligible transmission penalties at high gain values and improved robustness to WDM channels add-drop operations. BER measurements with bit rate of 10 Gb/s point out that the transmission penalties induced by pump-to-signal RIN transfer and DRS noise are suppressed below 0.5 dB up to very high net gain value of 20 dB. Optical measurements with the time-domain-extinction method [3] and theoretical predictions confirm that transmission penalties, observed at gain higher than 20 dB, are now mainly due to DRS noise rather than RIN transfer. Moreover, the dynamic behavior of the RRFO-based amplifier, which has been investigated both theoretically and experimentally under WDM channels add-drop operations, points out improvement in signal power transients in terms of overshoot, undershoot, and gain excursion.

II. EXPERIMENTAL SETUP

Fig. 1(a) shows the schematic diagram of the newly proposed RRFO. A 2-km-long spool of HNLF (effective area: $9.5 \mu\text{m}^2$) is counterpumped by a high-power fiber Raman laser at 1360 nm. With an FBG filter centered at 1450 nm (1-nm bandwidth) and a three-port optical circulator (OC), a narrow band of the amplified spontaneous emission (ASE) light is selected to circulate in counterpropagating direction, providing a fiber ring laser at 1450 nm. Eight 100-GHz-spaced WDM channels in *C*-band (ITU grid 1550.9–1556.5 nm) are coupled into the HNLF via

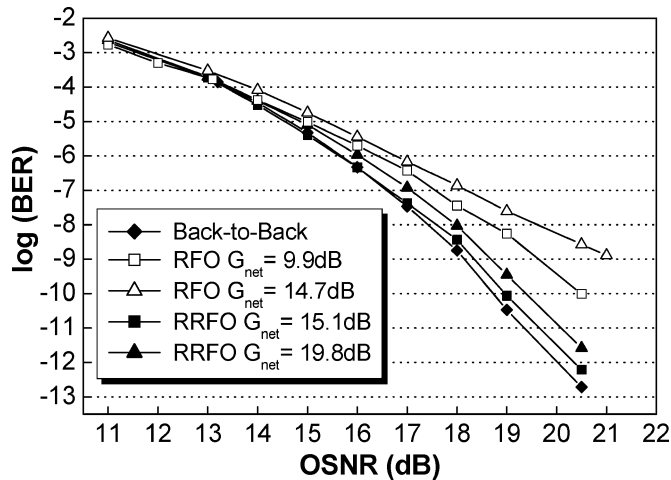


Fig. 2. BER measurements at 10 Gb/s versus OSNR for the RFO and RRFO schemes.

WDM1 coupler, amplified by the counterpropagating lasing light at 1450 nm, and then extracted by WDM2 at the amplifier output.

Fig. 1(b) shows a schematic diagram of the RFO [2] which has been characterized for comparison. The lasing light at 1450 nm is now generated within the HNLf spool by introducing two in-line FBGs, and propagates in both co- and counterdirections.

Transient effects are investigated by switching ON and OFF seven out of eight WDM channels by an acousto-optic modulator which reproduces WDM channels add-drop operations at the amplifier input [4].

III. THEORETICAL AND EXPERIMENTAL RESULTS

The RRFO performance has been first characterized in terms of net gain (G_{NET}), optical noise figure (NF), and saturated output power, considering eight 100-GHz-spaced WDM channels. The amplifier loss at 1550 nm is 2.2 dB, and the small signal net gain goes up to 20 dB with pump power $P_p = 800$ mW. The 3-dB saturated output power is more than 17 dBm with pump power $P_p = 640$ mW. Note that the OC in Fig. 1(a) is for C-band applications; much lower pump power would be required by using an OC with lower losses at 1450 nm. The optical NF remains below 4.5 dB for G_{NET} lower than about 20 dB and then starts to be degraded, likely by single backscattered ASE light increase.

BER measurements at 10 Gb/s versus received optical signal-to-noise ratio (OSNR) have then been carried out for both amplifier schemes, keeping the signal power constant at the receiver. The eight multiplexed WDM channels are modulated by a LiNbO₃ Mach-Zehnder modulator and decorrelated by using 1-km dispersion-compensating fiber (DCF) spool before being coupled into the HNLf. Back-to-back BER measurements versus received OSNR have been performed using DCF and HNLf spools with the 1360-nm pump OFF.

Fig. 2 shows the measured BER versus OSNR for both amplifiers at different net gain values. We can clearly see that the RFO amplifier performance is significantly degraded even at low G_{NET} values of 10–15 dB. In contrast, the newly proposed

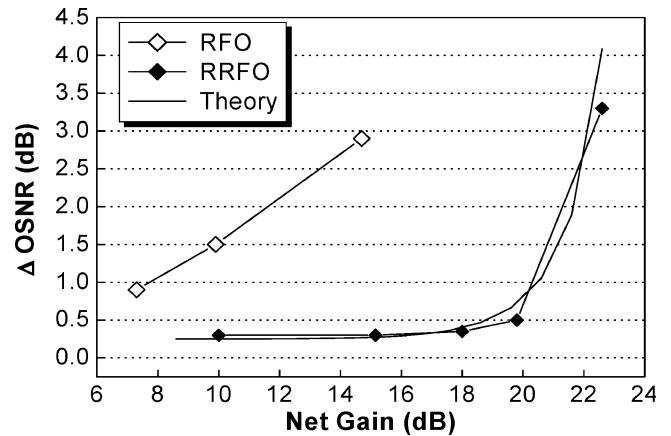


Fig. 3. OSNR penalty versus net gain G_{NET} for the RFO and RRFO schemes.

RRFO structure shows almost penalty-free transmission up to about 20 dB.

This is confirmed by the results of Fig. 3 where the OSNR penalty (ΔOSNR) in decibels versus net gain is shown. ΔOSNR is defined as the increment of OSNR required to obtain a given BER value, with respect to back-to-back. Considering a fixed BER = 10^{-9} , we can notice almost negligible OSNR penalties for the RRFO amplifier up to a net gain of about 20 dB.

Note that Fig. 3 also shows the computed OSNR penalty (ΔOSNR) induced by DRS noise. The relative impact of DRS noise-induced multipath interference (MPI) and ASE noise on the optical receiver performance has been studied using the Q -factor analysis proposed in [4], where it is assumed that the beat noise due to MPI and ASE on the receiver is the dominant contribution

$$Q = \frac{C}{\sqrt{\frac{1}{\text{OSNR}} + \frac{k}{\text{OSNR}_{\text{DRS}}}}} \quad (1)$$

where OSNR is the OSNR due to output ASE light, OSNR_{DRS} is the signal to DRS noise ratio, k is a factor dependent on the transmission format, and C is assumed to be constant. The ASE resolution bandwidth is 0.1 nm and the k -factor is assumed to be 1.89, corresponding to nonreturn-to-zero modulation format. Factor C in (1) has been estimated by fitting the back-to-back receiver characterization versus OSNR ($C = 0.74$). The theoretical calculation based on (1) has been performed using the OSNR_{DRS} shown in Fig. 4, measured by using a modified time-domain-extinction method. For each net gain value and corresponding OSNR_{DRS} , (1) has been used to calculate the OSNR required to ensure a Q -factor corresponding to a given BER value of 10^{-9} . The OSNR penalty is then easily computed as the difference between this required OSNR and the corresponding value in back-to-back conditions.

It is evident from Fig. 3 that the theoretical results well predict the measured OSNR penalty in case of RRFO-based amplifier, confirming that the penalty ΔOSNR at $G_{\text{NET}} > 20$ dB can be attributed to DRS noise. Actually this is consistent with the measured OSNR_{DRS} at $G_{\text{NET}} > 20$ dB, shown in Fig. 4, which reaches values below 25 dB starting to induce transmission penalty [5]. Note that the RRFO amplifier performance at

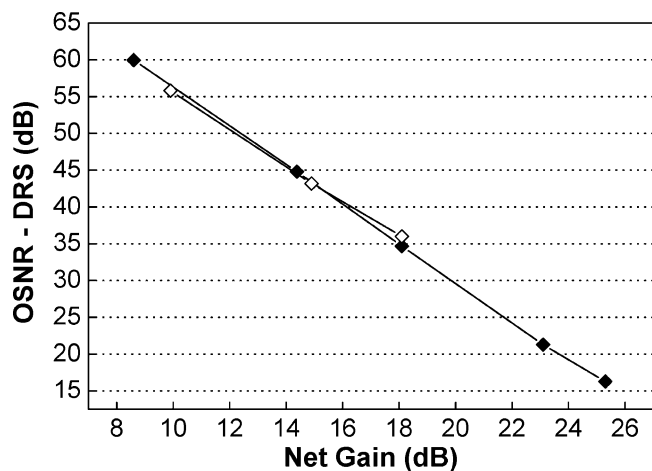


Fig. 4. OSNR due to the signal DRS versus net gain G_{NET} for the RRFO (solid square) and RFO (open square) amplifier schemes.

$G_{\text{NET}} > 20$ dB is also degraded in terms of optical NF, due to single backscattered ASE light. However, the penalty ΔOSNR does not describe this feature, being related only to transmission effects. Since the DRS noise measured for the RFO-based amplifier was almost the same as in the RRFO structure (shown in Fig. 4), the strong OSNR penalty observed in Fig. 3 for the RFO can be clearly ascribed to the RIN transfer from the copropagating part of lasing light at 1450 nm to the WDM signals.

We have finally investigated the transient behavior of both amplifier structures in Fig. 1, by switching ON and OFF seven out of eight WDM channels to reproduce WDM channel add-drop operations at the amplifiers input [4]. The surviving channel at 1550.9 nm is filtered out at the amplifier output and detected by a photodiode and digital oscilloscope. Also a theoretical analysis has been performed, based on the Raman amplifier dynamic model presented in [6], and suitably adapted to deal with resonant light generated at the pump wavelength in the RFO's based amplifier structures (RFO and RRFO). Fig. 5 compares the measured and computed output signal power transients at 1550.9 nm, induced by the drop and following add of the other seven channels, at different input signal power levels. We can clearly note a good quantitative agreement between theory and experiment for both the RFO and RRFO-based amplifiers and very limited signal power excursion even at high total input signal power levels.

Comparing these results with typical signal power transients present in longer conventional DRAs points out much faster transient response and also a sensible reduction in the output signal power overshoot [2]. Moreover, the newly proposed RRFO amplifier shows even lower output signal power excursions compared to the RFO amplifier operating at the same total input power. At the same time, the hazardous overshoots and undershoots following drop and add operations, respectively, were almost completely suppressed. This

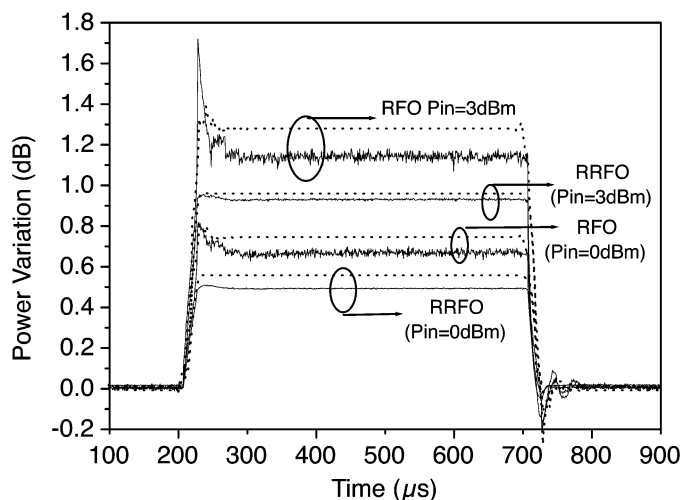


Fig. 5. Measured (solid line) and computed (dotted line) output signal power transients at 1550.9 nm for both RFO and RRFO amplifier structures.

is likely due to the fact that in case of RRFO, all lasing light is counterpropagating with respect to the WDM signals; as a consequence, fast lasing light variations induced by WDM channels add-drop operations are not directly transferred to the signals but mediated by the amplifier transit time. On the other hand, in case of RFO, part of the lasing light is copropagating and its variations can then be instantaneously transferred to the WDM signals.

IV. CONCLUSION

We have proposed a new second-order counterpumped RRFO scheme for discrete optical amplifier which provides high gain with negligible penalties. With the improved properties in terms of RIN transfer and reduced signal power transients, the newly proposed high gain and low noise RRFO can be attractive candidate for the next-generation discrete optical amplifier.

REFERENCES

- [1] M. N. Islam, "Raman amplifiers for telecommunications," *IEEE J. Sel. Topics Quantum Electron.*, vol. 8, no. 3, pp. 548–559, May/June 2002.
- [2] S. S.-H. Yam, M. E. Marhic, Y. Akasaka, K. Shimizu, N. Kikuchi, and L. G. Kazovsky, "Raman fiber oscillator as optical amplifier," *IEEE Photon. Technol. Lett.*, vol. 16, no. 6, pp. 1456–1458, Jun. 2004.
- [3] S. A. E. Lewis, S. V. Chernikov, and J. R. Taylor, "Characterization of double Rayleigh scattering noise in Raman amplifiers," *IEEE Photon. Technol. Lett.*, vol. 12, no. 5, pp. 528–530, May 2000.
- [4] G. Sacchi, S. Sugliani, G. Bolognini, S. Faralli, and F. Di Pasquale, "Experimental analysis of gain clamping techniques for lumped Raman amplifiers," in *Proc. ECOC 2003*, Rimini, Italy, Sep. 2003, Paper Tu3.2.4.
- [5] J. Bromage, L. E. Nelson, C. H. Kim, P. J. Winzer, R.-J. Essiambre, and R. M. Jopson, "Relative impact of multiple-path interference and amplified spontaneous emission noise on optical receiver performance," in *Proc. OFC 2002*, Anaheim, CA, Mar. 2002, Paper TuR3.
- [6] G. Bolognini and F. Di Pasquale, "Transient effects in gain-clamped discrete Raman amplifier cascades," *IEEE Photon. Technol. Lett.*, vol. 16, no. 1, pp. 66–68, Jan. 2004.